

Subnuclear localization and Cajal body targeting of transcription  
elongation factor TFIIS in amphibian oocytes

Abigail J. Smith\*, Yan Ling and Garry T. Morgan

Institute of Genetics, University of Nottingham, Nottingham NG7 2UH,  
UK

\*Current address:

Department of Biochemistry  
University of Bristol  
School of Medical Sciences  
Bristol BS8 1TD  
UK

Running title: TFIIS localization in oocyte nuclei

Author for correspondence:

Garry T. Morgan  
Institute of Genetics  
University of Nottingham  
Queens Medical Centre  
Nottingham NG7 2UH  
UK  
Tel: +44 (115) 970 9402  
Fax: +44 (115) 970 9906  
Email: [garry.morgan@nottingham.ac.uk](mailto:garry.morgan@nottingham.ac.uk)

Keywords: lampbrush chromosomes, RNA polymerase II, germinal vesicle, SII,  
*Xenopus*.

## ABSTRACT

We have examined the localization and targeting of the RNA polymerase II (pol II) transcription elongation factor TFIIS in amphibian oocyte nuclei by immunofluorescence. Using a novel antibody against *Xenopus* TFIIS the major sites of immunostaining were found to be Cajal bodies, nuclear organelles that also contain pol II. Small granular structures attached to lampbrush chromosomes were also specifically stained but the transcriptionally-active loops were not. Similar localization patterns were found for the newly-synthesised *myc*-tagged TFIIS produced after injection of synthetic transcripts into the cytoplasm. The basis of the rapid and preferential targeting of TFIIS to Cajal bodies was investigated by examining the effects of deletion and site-specific mutations. Multiple regions of TFIIS contributed to efficient targeting including the domain required for its binding to pol II. The localisation of TFIIS in Cajal bodies, and in particular the apparent involvement of pol II binding in achieving it, offer further support for a model in which Cajal bodies function in the pre-assembly of the transcriptional machinery. Although our findings are therefore consistent with TFIIS playing a role in early events of the transcription cycle they also suggest that this elongation factor is not generally required during transcription in oocytes.

## INTRODUCTION

The giant nucleus or germinal vesicle (GV) of an amphibian oocyte provides particularly favourable material with which to address basic questions concerning the relationship between the processes of gene expression and nuclear organization. GVs exhibit a range of structures with extraordinary levels of morphological detail, the best known of which are lampbrush chromosomes (reviewed in Callan, 1986; Morgan, 2002). These are structures that display extended chromatin loops on which the actively transcribed regions of the genome can be resolved in cytological preparations. The events and molecular components associated with the elongation stage of transcription are therefore amenable to study *in situ*. Recently it has proved possible to investigate by immunostaining the disposition in lampbrush chromosome loops of elongation complexes containing either RNA polymerase II (pol II) or pol III, and in the former case to detect particular phosphoisomers of the carboxy-terminal domain (CTD) of the largest subunit (Gall *et al.*, 1999; Morgan, 2002; Murphy *et al.*, 2002; Doyle *et al.*, 2002). However, pol II is also found in the GV in transcriptionally-inactive structures. Amphibian GVs contain 50-100 organelles that are equivalent to the Cajal bodies (CBs) first identified in somatic cells (Gall *et al.*, 1995) and both immunostaining and the targeting of epitope-tagged subunits have firmly established that oocyte CBs contain pol II (Gall *et al.*, 1999; Morgan *et al.*, 2000; Doyle *et al.*, 2002). Similar approaches have shown that pol I and pol III are also present in oocyte CBs (Gall *et al.*, 1999; Murphy *et al.*, 2002). In addition oocyte CBs contain pol II transcription initiation factors and components required for the processing of various types of nuclear transcript (reviewed in Gall, 2000).

Since CBs are conserved in plant and animal nuclei their cellular functions are likely to be fundamental and roles in the transport and modification of RNA processing machineries have been suggested (reviewed in Matera, 1999; Dundr and Misteli, 2001). However a recent and wider-ranging model for CB function (Gall *et al.*, 1999; Gall, 2000) proposes that the three types of nuclear RNA polymerase are assembled in CBs and that each associates there with their cognate transcription initiation factors and RNA processing complexes to generate multifunctional molecular machines, transcriptosomes, that are then transported to transcription sites. As well as accounting for the many different components detected in CBs, the transcriptosome model is consistent with recent findings from biochemical and genetical approaches that suggest the assembly of pol II holoenzymes and their association with various RNA processing components prior to transcription (reviewed in Myer and Young, 1998; Hirose and Manley, 2000).

In order to investigate further the interrelationships between nuclear organization and the pol II transcription cycle we have studied a type of transcriptional component that has not previously been examined in this respect, namely an elongation factor, TFIIS (also known as SII). TFIIS increases overall pol II transcription rates in *in vitro* biochemical assays by reactivating elongation complexes whose progress has been blocked by a variety of impediments (reviewed in Wind and Reines, 2000). TFIIS binds directly to pol II and is thought to exert its effect by both activating an intrinsic pol II transcript cleavage activity and stimulating the arrested elongation complex to re-initiate chain elongation. TFIIS thus allows repeated attempts by stalled pol II eventually to pass through a transcription block. Although the structure and biochemical properties of TFIIS are known in detail (reviewed in Wind and Reines, 2000 and

summarised in Fig. 1), its *in vivo* role is poorly understood. In particular it is not established that TFIIS functions in the relief of transcriptional arrest *in vivo*, nor at what stage(s) of the transcription cycle it is associated with pol II. For instance, an involvement of TFIIS prior to initiation has been inferred from its use in protein-affinity chromatography as a ligand to bind initiation-competent pol II holoenzyme complexes that contain general transcription factors (Pan *et al.*, 1997) and RNA processing factors (Robert *et al.*, 2002).

We show here that TFIIS is localized in oocyte CBs and that its efficient targeting to CBs requires, amongst other regions, its pol II-binding site. Our findings both suggest a pre-transcriptional role for TFIIS and provide evidence for a basic prediction of the transcriptosome model of CB function, namely that the interaction of pol II with other elements of the transcription machinery occurs in CBs. However, our inability to detect TFIIS convincingly in actively-transcribing lampbrush chromosome loops suggests that it is not normally a part of pol II transcription elongation complexes.

## MATERIALS AND METHODS

### Expression constructs

Full-length cDNA clones encoding *Xenopus* TFIIS, namely po2 (Plant *et al.*, 1996), xTFIIS.oB (Labhart and Morgan, 1998), and xTFIIS.l (Labhart, 1997), were used to create *myc*-tagged TFIIS constructs in two ways. In the first approach, which was used to make constructs *myc*-UTR-xIIS and pcx1, fragments containing the coding region and flanking untranslated regions from po2 and xTFIIS.l, respectively, were first cloned into the *myc*-tag vector MT-6D

(Tuma *et al.*, 1993) and then into pcDNA3 (Invitrogen Life Technologies, Paisley). Each insert encodes a fusion protein comprising six tandem copies of a 13-amino acid repeat containing the *myc* epitope, a 21- (*myc*-UTR-xIIS) or 24- (*pcxl*) amino acid spacer derived from 5' UTR sequence and then the complete xTFIIS coding region. In the second approach, which was used to create the *myc*-tagged full-length construct *myc*-xIIS and its mutant derivatives, restriction sites were introduced during polymerase chain reaction (PCR) generation of TFIIS cDNA fragments in order to allow insertion of just the desired reading frame into *myc*-tag vectors. The vectors used were based on pcDNA3 into which we had inserted either the 6-*myc* tag from MT-6D or a modified tag in which the SV 40 nuclear localization signal (NLS), PPKKKRKV, replaces the sixth *myc* repeat (Wu *et al.*, 1994).

Site-directed mutagenesis of xTFIIS.o was accomplished by PCR on pcO2b using *Pfu* Turbo DNA polymerase (Stratagene, La Jolla CA) and mutagenic primers that encoded the amino acid substitutions indicated in Fig. 8. Inserts were recloned into the above *myc*-tag vectors. For expression of a glutathione S-transferase (GST)-xTFIIS fusion protein in *E. coli*, a PCR fragment encoding amino acids 1-80 of xTFIIS.oB was cloned into pGEX-4T-1 (Amersham Pharmacia Biotech UK Ltd, Little Chalfont) to form construct pGEX-xIIS1-80. DNA sequencing verified that the desired reading frame was present in each construct.

#### TFIIS expression and antibody production

Construct pGEX-xIIS1-80 was expressed in *E. coli* strain JM105 and the fusion protein purified using glutathione agarose (Sigma Chemical Co., St Louis MO) according to the manufacturer's instructions. The affinity-purified GST-xTFIIS<sup>1-80</sup> fusion protein was used to

immunise a rabbit as a 1:1 emulsion with Freund's Complete Adjuvant (FCA). Five follow-up boosts with antigen mixed 1:1 with FCA were carried out at 14 day intervals until maximum titre of serum 37X was obtained.

#### Expression of *myc*-tagged xTFIIS in oocytes

Oocytes were obtained from *Xenopus laevis* or *Triturus vulgaris* (both supplied by Blades Biological; Edenbridge, Kent) and used to express TFIIS from synthetic transcripts that were injected into the cytoplasm. Capped sense-strand transcripts were prepared using a mMessage mMachine kit (Ambion Inc., Austin TX) according to the manufacturer's instructions to transcribe linearised plasmid DNAs with T7 RNA polymerase. RNAs were resuspended in RNase-free H<sub>2</sub>O and their relative concentrations and sizes checked by agarose gel electrophoresis. For *Xenopus*, separated oocytes were prepared from small ovary fragments by treatment with 1 mg/ml collagenase (Type II; Sigma) in calcium-free OR2 saline (82.5 mM NaCl, 2.5 mM KCl, 1 mM MgCl<sub>2</sub>, 1 mM Na<sub>2</sub>HPO<sub>4</sub>, 5 mM HEPES) for about an hour, followed by rinsing in OR2 containing 1 mM CaCl<sub>2</sub>. Separated *Triturus* oocytes were obtained by manual dissection in OR2. After overnight incubation in OR2 at 18°C, healthy-looking stage IV or V *Xenopus* oocytes and *Triturus* oocytes 0.8-1.0 mm in diameter were injected with 25 nl of RNA (1 µg/µl) and incubation continued for the periods stated in the text.

#### Immunoblotting

GV extracts for blotting were prepared by manually dissecting oocytes in GV isolation medium (83 mM KCl, 17 mM NaCl, 6.5 mM Na<sub>2</sub>HPO<sub>4</sub>, 3.5 mM KH<sub>2</sub>PO<sub>4</sub>, 1 mM MgCl<sub>2</sub>, 1mM DTT; pH 7.0-7.2) and collecting GVs, each in 2µl of the same medium, into pools of 5-10. 10 µl

SDS-loading buffer (200mM TrisCl pH6.8, 400mM DTT, 8% SDS, 0.4% bromophenol blue, 40% glycerol) was added to each pool and the samples stored at -80°C. HeLa cell extracts were prepared from cells previously transfected with xTFIIS constructs using Effectene (QIAGEN Ltd., Crawley) according to the manufacturer's instructions. Control samples of *myc*-tagged TFIIS fusion proteins were obtained by coupled *in vitro* transcription/translation using the TnT T7 Quick system (Promega Corp., Madison WI).

Protein samples were blotted using standard procedures (Harlow and Lane, 1999) prior to incubation with either of the primary antibodies, rabbit serum 37X (1:1000 dilution) or the anti-*myc* mouse IgG monoclonal antibody 9E10 (Evan *et al.*, 1985) at 2.5 µg/ml. Following subsequent incubation with the appropriate horseradish peroxidase-conjugated goat secondary antibody (Amersham Pharmacia Biotech; 1:2500 dilution), detection was performed using an enhanced chemiluminescence (ECL) kit (Amersham Pharmacia Biotech).

#### Preparation of GV spreads

GVs from injected or uninjected oocytes were manually dissected into GV isolation medium as above. Cytological spread preparations of *Xenopus* GV contents were made essentially according to the procedure developed in the laboratory of Professor J. G. Gall (Gall *et al.*, 1991; Gall *et al.*, 1999). *Triturus* GV spreads were made in a similar fashion except that the medium used to disperse the nuclear gel contained paraformaldehyde at 0.01% instead of 0.1% and centrifugation to attach the spread GV contents to the base of the observation chamber was carried out at 2,500g rather than 5,000g. After centrifugation the base of the observation chamber bearing the GV spread was removed and the preparation fixed for an hour in 2%

paraformaldehyde made up in phosphate buffered saline (PBS: 137mM NaCl, 2.7mM KCl, 10.2mM Na<sub>2</sub>HPO<sub>4</sub>, 1.8mM KH<sub>2</sub>PO<sub>4</sub>, pH7.4) containing 1 mM MgCl<sub>2</sub>.

#### Immunostaining and fluorescence microscopy

Immunostaining of GV spreads was performed essentially as described by Gall *et al* (1991) using primary antibodies diluted as follows: rabbit polyclonal serum 37X against xTFIIS, 1:500 dilution; rabbit polyclonal serum  $\alpha$ p80 against coilin (a gift from Professor A. Lamond, University of Dundee) 1:350 dilution; mAb 9E10 (Boehringer Mannheim Corp., Indianapolis IN), 1  $\mu$ g/ml; H14 (Warren *et al.*, 1992), a mouse IgM mAb against the phosphorylated CTD of RNA pol II, undiluted culture supernatant. Preparations were then incubated with the appropriate secondary antibody diluted as follows: Cy3-conjugated (Jackson ImmunoResearch Laboratories) or FITC-conjugated (Santa Cruz Biotechnology, Inc., Santa Cruz CA) goat anti-rabbit IgG 2 $\mu$ g/ml; Alexa 488-conjugated goat anti-mouse IgG (Molecular Probes Europe BV, Leiden), 5 $\mu$ g/ml; Cy3-conjugated (Chemicon International Inc., Temecula CA) or Alexa 594-conjugated (Molecular Probes) goat anti-mouse IgM, 1-2  $\mu$ g/ml. Preparations were mounted in 50% glycerol/PBS except for those stained with FITC, which were mounted in 50% glycerol/SlowFade-Light (Molecular Probes).

An Olympus BX-60 microscope (Olympus Optical Co. (U.K.) Ltd, London) was used for differential interference contrast (DIC), phase contrast and fluorescence microscopy. Filter set 41001 (Chroma Technology Corp., Brattleboro VT) was used to detect FITC and Alexa 488 fluorescence, filter set 41002b (Chroma Technology Corp.) was used for Cy3 fluorescence and filter set 41004 (Chroma Technology Corp.) was used for Alexa 594. Images were captured with

a Princeton Instruments digital CCD camera (Roper Scientific, Tucson AZ) using IPLab software (Scanalytics Inc, Fairfax VA) and processed with Adobe Photoshop (Adobe Systems Inc., San Jose CA).

## RESULTS

### (1) Specific detection of the xTFIIS.o isoform in *Xenopus* germinal vesicles

In both mammals and amphibians the TFIIS gene family encodes three distinctive isoforms whose mRNAs exhibit characteristic expression patterns (Labhart and Morgan, 1998; Taira *et al.*, 1998). In *Xenopus* oocytes xTFIIS.o mRNA is abundant, TFIIS.l mRNA is present at low levels and TFIIS.h mRNA is undetectable (Labhart and Morgan, 1998), although there is no information regarding the relative abundance of the proteins themselves. We wanted to raise a rabbit polyclonal antibody specifically against xTFIIS.o and so generated an antiserum, 37X, against a GST fusion protein containing the N-terminal 80 amino acids of xTFIIS.oB (Plant *et al.*, 1996). This region of TFIIS comprises a complete structural domain (Booth *et al.*, 2000) but shows a greater inter-isoform amino acid sequence divergence than the C-terminal region (Fig. 1). We initially tested whether serum 37X could specifically detect xTFIIS by immunoblotting extracts of HeLa cells that had been transfected with various *myc*-tagged xTFIIS.o expression vectors. Those xTFIIS.o polypeptides that included the N-terminal region were clearly detected by the antiserum and produced bands of about the expected molecular weight (Fig. 2A). However, polypeptides that lacked this region were not detected by the serum although their presence in the extracts could clearly be demonstrated by immunoblotting with an antibody

against the *myc* epitope (data not shown). The specificity of serum 37X was also suggested by the absence of any other cross-reacting proteins in these HeLa extracts including endogenous human TFIIIS, which is readily-detectable using an antiserum produced against hTFIIIS.o (unpublished observations).

We next immunoblotted protein extracts prepared from the manually-isolated GVs of *Xenopus* oocytes that either were uninjected or had expressed *myc*-tagged xTFIIIS.o or xTFIIIS.l from injected transcripts. In all the GV extracts (Fig. 2B) serum 37X reacted with a band of approximately 35 kDa that corresponds closely to the size expected for endogenous xTFIIIS.o. The serum also reacted strongly with full length *myc*-tagged xTFIIIS.o and some of its minor degradation products but not with *myc*-tagged xTFIIIS.l, which we know was present in the extract (data not shown). The lack of any other cross-reacting endogenous proteins in *Xenopus* GV extracts also indicates that the xTFIIIS.h isoform, which is about twice the size of the other two (Taira *et al.*, 2000) is either, like its mRNA, not present at detectable levels in oocytes or if present does not cross-react with serum 37X. Overall our immunoblotting results suggest that serum 37X allows the specific detection of the N-terminal region of the xTFIIIS.o isoform in *Xenopus* GVs.

(2) xTFIIIS.o is present in Cajal bodies and chromosome granules

Cytological preparations of GVs from amphibian oocytes provide nuclear structures that can be examined in great detail by conventional light microscopy (examples shown in Fig. 3). In addition to lampbrush chromosomes three types of globular object are routinely observed in GV

spreads from *Xenopus* oocytes (Gall, 1992; Gall *et al.*, 1999). These are extrachromosomal nucleoli, Cajal bodies (CBs) and B snurposomes, some of which can be associated with CBs, either attached to the surface or as inclusions completely embedded within the CB matrix. We immunostained *Xenopus* GV spreads with serum 37X at a range of dilutions up to 1:1000. At all dilutions CBs were intensely stained and were the most prominent stained objects in the spreads (Fig. 3A) while at the same dilutions the 37X pre-immune serum gave no specific staining of any object. Only the matrix of the CB was brightly stained by serum 37X with any associated B snurposomes being much fainter, and this gave rise to a pattern of staining found also for other CB components such as the CB marker protein p80 coilin (Fig. 3B). Free B snurposomes, like CB-associated ones, were only faintly stained with serum 37X as were extrachromosomal nucleoli (Fig. 3A, C). We double-stained some GV preparations with serum 37X and mAb H14, which is highly specific for the phosphorylated pol II CTD and has been shown to stain CBs and loop axes (Gall *et al.*, 1999; Morgan *et al.*, 2000; Doyle *et al.*, 2002). Co-staining with mAb H14 both demonstrated the co-localization of pol II and TFIIS in CBs and identified unambiguously those CBs that were not morphologically distinctive (Fig 3D). It also emphasised a consistent feature that we noted in all of the GV spreads immunostained with serum 37X; namely that the staining of lampbrush chromosomes was weak (Fig. 3E ) and what little there was seemed to reflect the general distribution of loop matrix rather than showing the strong staining of loop axes observed with pol II antibodies (Fig. 3E). The weak staining of loops, B snurposomes and nucleoli, which on the basis of pixel values in the images captured by a CCD camera we estimate to be an order of magnitude less than that of the CB matrix, could indicate the presence of small amounts of TFIIS in these structures. Alternatively it could represent the residual association

of soluble TFIIS from the nucleoplasm, most of which is washed off during GV spread preparation.

We also observed that as well as CBs, structures of a second type were strongly and specifically immunostained by serum 37X. These structures are small (1-2  $\mu\text{m}$  diameter) near-spherical proteinaceous granules that are regularly attached to the axes of lampbrush chromosomes at either interstitial or terminal loci (reviewed in Callan, 1986; Morgan, 2002). Although their functional significance is unclear, in *Xenopus laevis* these granules serve for chromosome recognition, with terminal granules occurring at one end of 15 of the 18 lampbrush chromosomes. Figure 3C shows immunostaining of terminal granules by serum 37X. Since immunostaining and targeting experiments have shown that pol II occurs in *Xenopus* granules (Gall and Murphy, 1998; Morgan *et al.*, 2000; Morgan, 2002), their staining with serum 37X re-emphasises the fine-scale co-localization of TFIIS.o and pol II in GVs and the presence of both in transcriptionally-inactive structures.

### (3) *myc*-tagged TFIIS.o is targeted to CBs and chromosome granules

A second approach that has been used productively to investigate the subnuclear localization of polypeptides in GVs is based on the targeting of epitope-tagged fusion proteins that have been translated from synthetic capped transcripts injected into the oocyte cytoplasm. We constructed two *myc*-tagged versions of xTFIIS.o for this purpose, *myc*-UTR-xIIS and *myc*-xIIS (see Materials and Methods), and although the former gave higher levels of protein both gave similar localisation patterns. We showed firstly by immunoblotting extracts of manually-dissected GVs

that *myc*-tagged TFIIIS.o is made and successfully transported to the nucleus in injected oocytes. Figure 4A shows that a band with a slightly lower mobility than expected for *myc*-xIIS (44.4 kDa) is easily detected by mAb 9E10 in GV's after just 4h of incubation. With longer incubations more *myc*-xIIS accumulated in the GV (Fig. 4A) and by 24 h we estimate from an immunoblot with serum 37X (Fig. 2B) that the amount of *myc*-tagged TFIIIS.o in the GV is several fold higher than that of endogenous TFIIIS.o.

We then immunostained GV spreads from *Xenopus* oocytes that had been injected with *myc*-xIIS transcripts and incubated for 4 - 48 h. At even the shorter time points CBs were brightly and specifically stained by mAb 9E10 (Fig. 4B) and the pattern was maintained over longer incubations (Fig. 4C). Immunostaining of preparations from uninjected oocytes failed to reveal any specific CB labelling (Fig. 4C). As well as the intense staining of CBs, other structures were detectably stained by mAb 9E10 (Fig. 4C,D) and this was especially apparent in oocytes that produced higher levels of *myc*-tagged protein, such as those expressing construct *myc*-UTR-xIIS. Nucleoli, lampbrush chromosomes and B snurposomes were all stained faintly by mAb 9E10 but, as estimated by representative pixel values in the image, the staining was at a several-fold lower level than that of CBs in the same spread. However, terminal and axial chromosome granules did appear to contain higher levels of *myc*-tagged TFIIIS.o (Fig. 4D). Despite their small size the granules stood out as being much more brightly stained by mAb 9E10 than were neighbouring B snurposomes and nucleoli. Overall since the targeting patterns of *myc*-tagged TFIIIS.o were essentially the same as the localization patterns determined for endogenous TFIIIS.o by immunostaining, we conclude that those structures that appear strongly positive in

both assays, namely CBs and chromosome granules, are genuine sites of TFIIS accumulation *in vivo*.

The extent to which *myc*-tagged TFIIS was present in the other GV structures was more difficult to establish reliably since their weak but detectable staining could indicate a low-level targeting of TFIIS. However, it could also be that this generalised staining is caused by a non-specific sticking of the overexpressed *myc*-tagged TFIIS from the nucleoplasm to the surfaces of these objects during spread preparation. We thought it particularly important to address the apparent lack of specific loop targeting by TFIIS and so we also investigated targeting in the oocytes of a newt, *Triturus vulgaris*. Lampbrush chromosomes from newt oocytes exhibit more extended loops than do anurans such as *Xenopus* and the loop axes also immunostain more intensely for pol II (Gall and Murphy, 1998). Therefore newt lampbrush chromosomes potentially offer the opportunity to assess targeting of transcriptional proteins at improved levels of resolution and sensitivity. (Unfortunately serum 37X gave non-specific staining of newt GV spreads, we think because of the high specificity of the antiserum for *Xenopus* TFIIS.o, and so we were unable to determine the localization of endogenous newt TFIIS). *Triturus* oocytes were used to express *myc*-UTR-xIIS for periods between 21-43 h and then GV spreads were prepared and stained with mAb 9E10. At all time points CBs were intensely stained, both the majority that exist free in the nucleoplasm as well as those much larger and complex CBs that are regularly attached at two chromosomal loci in this species. Figure 5 shows an example of the intense mAb 9E10 staining of a complex chromosomal CB and in contrast the considerably weaker staining (about 10-fold less judging from representative pixel values) of nearby giant loop-related structures. Moreover,

just like nucleoli and B-snurposomes, typical lateral loops were only weakly stained and even this staining reflected the mass of the RNP matrix rather than being confined to the loop axis.

We confirmed that we were able to detect the specific targeting of *myc*-tagged proteins to loops by repeating the experiment of Jantsch and Gall (Jantsch and Gall, 1992) involving the U1 snRNP C protein. Using construct pCMA (Jantsch and Gall, 1992) to produce transcripts encoding *myc*-tagged C protein we found that this fusion was targeted efficiently to loops where it resulted in strong mAb 9E10 staining of loop matrices (Fig. 5). Therefore we conclude that in both *Xenopus* and newt oocytes exogenous *myc*-tagged TFIIS is not specifically targeted to actively-transcribed regions, although targeting to CBs is clearly conserved between anurans and urodeles. We have also found that *myc*-tagged human TFIIS.o is as efficiently targeted to CBs in *Xenopus* oocytes as is xTFIIS.o (unpublished observations). It seems likely therefore that any sequence(s) in TFIIS required for CB targeting is well conserved.

#### (4) Multiple regions of TFIIS contribute to efficient CB targeting

We utilised deletion constructs of xTFIIS in order to determine whether the polypeptide possessed a localized, dedicated CB targeting signal or whether dispersed, multifunctional domains were involved. In the first instance the constructs were based upon dividing TFIIS into three segments according to the broad patterns of sequence conservation exhibited by vertebrate TFIIS isoforms (Figs. 1 & 6). Regions of xTFIIS encoding these three polypeptide segments were fused downstream of both the *myc* epitope and a copy of the SV40 nuclear localization sequence (NLS), since we know from the behaviour of analogous constructs in HeLa cells that

the N-terminal segment is needed for efficient nuclear localization of TFIIIS (unpublished observations). Capped *in vitro* transcripts encoding each of the three fusion proteins as well as an NLS-tagged full-length xTFIIIS control were injected in parallel into the cytoplasm of *Xenopus* oocytes. Each construct was tested in at least two different batches of oocytes with GVs being isolated 24-48 h after injection and processed either for immunoblotting or for cytological spreads.

The results of immunoblotting with mAb 9E10 (Fig. 6B) showed that constructs containing each of the three isolated xTFIIIS segments were expressed in oocytes and were present in GVs at similar levels. GV spreads were either stained singly with mAb 9E10 or double-stained with 9E10 and anti-coilin antibodies. As before, specific targeting of the full-length myc-nls-xTFIIIS resulted in brightly-stained CBs and presumptive non-specific sticking to the surfaces of B-snurposomes gave rise to low-level staining (Fig. 6C). However, neither the TFIIIS N-terminal segment (amino acids 1-80), the C-terminal segment (amino acids 173-303) nor the internal L segment (amino acids 80-176) encoded by constructs myc-nls-xN, myc-nls-xC and myc-nls-xL, respectively, showed evidence of CB targeting (Fig. 6C). In GVs expressing these polypeptides the intensity of staining of CBs was similar to that of attached or adjacent B snurposomes, with the ratio of average pixel values sampled in CBs relative to B's being in the range 1-1.5 instead of the 2.5-3 found in parallel for the full-length control. These findings were consistent over a range of post-injection incubation periods and suggested that none of the three TFIIIS segments contained an active signal that could suffice for CB targeting. One possible explanation was that such a signal is only functional in the context of the intact protein, but this seemed unlikely in view of the structural studies of TFIIIS that suggest the individual domains fold both

independently of each other and regardless of the polypeptide context (Qian *et al.*, 1993; Morin *et al.*, 1996; Olmsted *et al.*, 1998).

It remained possible that a stand-alone CB targeting signal existed in TFIIS but that it was bisected by the deletion endpoints in the constructs examined above. This possibility was tested by examining the targeting of two other deletion constructs, myc-nls-xN+L and myc-nls-xC+L (Fig. 6A), in which two of the three xTFIIS segments were now contiguous. Again immunoblotting indicated that the constructs were efficiently expressed in GV's (Fig. 6B), although as with the full-length polypeptide some degradation of the fusions occurred, we think during GV processing. In GV spreads from oocytes injected with myc-nls-xN+L (amino acids 1-176) CBs appeared no more intensely stained by mAb 9E10 than did B snurposomes (Fig. 6C) and relative pixel values for the two structures appeared in the range found for the single TFIIS segments above. However, in oocytes expressing the fragment of TFIIS encoded by myc-nls-xC+L (amino acids 80-303) there was a degree of specific CB staining above background (Fig. 6C), although to different extents in different oocytes. In most spreads CB staining was approximately 1.5-2 times that of B snurposomes and was sometimes higher, indicating a degree of targeting that was above that of the other deletion constructs but distinctly below that of full length TFIIS. We interpret the restoration of some CB targeting to myc-nls-xC+L relative to the absence of targeting found for myc-nls-xC as being due to the reconstitution of TFIIS structural domain II, which contains the pol II binding region. This suggests that pol II binding contributes to CB targeting of TFIIS and this possibility is tested further below. In addition, since full length TFIIS (amino acids 1-303) showed much stronger targeting than myc-nls-xC+L (amino acids 80-303) this suggests that the N-terminal region also contributes to full CB targeting efficiency.

However it would appear that the targeting effect of the N-terminal region is insufficient to be detectable alone in the myc-nls-xN fusion.

Two further constructs were utilised to assess the contributions to targeting of other regions of TFIIS (Fig. 7A). We found in GV spreads made from oocytes injected with construct myc-xN+C that the intensity of CB immunostaining with mAb 9E10 was comparable to that obtained with full-length TFIIS in parallel injections (Fig. 7B). Since this deletion construct simply lacks the internal L segment (amino acids 81-172), the result suggests that this, the most variable region of TFIIS, is dispensable for CB targeting. The second construct, myc-UTR-xIIS $\Delta$ 232 (Fig. 7a), contains a premature stop codon after amino acid 232 and therefore encodes a C-terminally deleted TFIIS polypeptide. In GV spreads CBs from oocytes injected with myc-UTR-xIIS were much more intensely stained with mAb 9E10 than those expressing myc-UTR-xIIS $\Delta$ 232 (Fig. 7C). However, the estimated ratio of 2:1 for CB relative to B snurposome pixel values suggests that the reduction in CB targeting observed for myc-UTR-xIIS $\Delta$ 232 is somewhat less than that resulting from deletion of the N-terminal region in myc-nls-xC+L. Nonetheless our results suggest that a third region of TFIIS makes some contribution to efficient CB targeting.

#### (5) Mutation of the RNA polymerase II interacting region reduces CB targeting of TFIIS

In order to clarify the contributions that particular domains of TFIIS make to CB targeting, we carried out site-specific mutagenesis of residues known or predicted to affect TFIIS structure or function. In one mutant three conserved residues in the N-terminal region of xTFIIS were substituted (Fig. 8A). This mutation disrupts nuclear localization of TFIIS in HeLa cells

(unpublished observations) so in order to ensure high nuclear levels of the mutant protein in oocytes we included an SV40 NLS in the myc-tagged fusion protein, myc-NLS-xLW3. In another mutant, myc-xZR2, two of the four zinc-liganding cysteines in the zinc ribbon structural domain were replaced with alanine (Fig. 8A), a mutation that by destroying the metal binding site is expected to disrupt the entire structural domain. Finally, to create the mutant myc-xPOL2 two basic residues needed to mediate the binding of TFIIS to pol II (Fig.1) were substituted with acidic residues (Fig. 8A). Single alanine substitutions of the equivalent residues (see Fig. 1) in yeast TFIIS are known to reduce the affinity of its interaction with pol II at least 10-fold without affecting protein structure (Awrey *et al.*, 1998) and analogous alanine substitutions in human TFIIS severely disrupt its *in vitro* activities (Cipres-Palacin and Kane, 1995). Capped transcripts encoding the mutant myc-xTFIIS fusions were injected into *Xenopus* oocytes in parallel with wild type xTFIIS controls and immunoblotting of GV extracts from oocytes showed that the mutant and wild type proteins were expressed at comparable levels. In GV spreads specific staining of the CB matrices by mAb 9E10 was apparent for the mutants myc-NLS-xLW3 and myc-xZR2 (Fig. 8B) and by direct observation the intensity of staining appeared similar to that of wild type TFIIS. However, for the mutant myc-xPOL2 it was clear that there was often a marked reduction in CB staining relative to that found for control xTFIIS (Fig. 8B) and this was confirmed from estimates of the ratio of CB to B snurposome pixel values. The extent of the reduction in specific CB staining was somewhat variable both between oocytes and between duplicate injections (Fig. 8C) but overall many CBs showed little or no specific staining. We conclude that this mutation of the pol II binding site sufficiently disrupts the CB localization mechanism of TFIIS that its effect is detectable in our targeting assay.

## DISCUSSION

Immunostaining of endogenous TFIIS and the targeting of newly-synthesised TFIIS both suggest that in oocyte nuclei the principle structures in which this transcription factor is localized are CBs. Several recent studies of oocyte nuclei have revealed the presence of a variety of components of the pol II transcriptional machinery in CBs. These components include pol II subunits (Gall *et al.*, 1999 Morgan *et al.*, 2000 Doyle *et al.*, 2002), a subunit of the general transcription factor TFIIF (Gall *et al.*, 1999), the TBP subunit of TFIID (Gall, 2000) and the TBP-associated factor TAFII70 (Bucci *et al.*, 2001). At the least, the co-localization of the pol II-binding elongation factor TFIIS in the same structure as the aforementioned components is consistent with the transcriptosome model for CB function (Gall *et al.*, 1999; Gall, 2000), according to which CBs are the sites for the assembly of the nuclear gene expression machineries. However, as discussed below our studies of the CB targeting of TFIIS also provide support for a further requirement of the transcriptosome model, namely that there should be physical interactions between pol II and other transcriptional proteins in CBs.

We found that three regions of TFIIS contribute to efficient CB targeting. However, comparison of these regions with each other and with the targeting regions of other CB polypeptides (Wu *et al.*, 1994; Abbott *et al.*, 1999) do not reveal any common signal sequences for CB localization. Indeed it appears likely that subnuclear localization patterns in general are not reliant upon specific, discrete localization signals but on disparate intermolecular interactions with multiple targets, the aggregate effect of which is to cause a given protein to accumulate in particular nuclear compartments rather than continuing to diffuse freely in the nucleoplasm (Misteli, 2001).

It also seems that the continual dynamic interchange of polypeptides that comprise macromolecular complexes and subnuclear structures is a crucial feature underlying nuclear organization (Dundr and Misteli, 2001). We interpret CB targeting itself as reflecting rapid exchange of tagged TFIIS with endogenous TFIIS molecules that are normal CB components at steady state because of their presence in pol II transcription complexes or sub-complexes. Exchange has been proposed as the likely explanation for the targeting of another oocyte CB protein, the U1 snRNP-specific C protein (Jantsch and Gall, 1992). Superimposed on exchange with TFIIS in pre-assembled complexes, the targeting of tagged TFIIS to the CB might also reflect the incorporation during assembly of newly-synthesised, tagged TFIIS into pol II complexes in place of endogenous TFIIS.

The relatively detailed knowledge of the interactions between TFIIS and the transcription machinery (reviewed in Wind and Reines, 2000) enables some suggestions as to the mechanisms contributing to CB targeting. The effects of deleting either an N-terminal region of 80 amino acids or a similar sized C-terminal region containing the domain II/III linker region and the zinc ribbon domain revealed that both regions contributed to efficient CB targeting (see Fig.1 for a summary of TFIIS structural organization). Since the N-terminal region was previously implicated in binding to a pol II holoenzyme (Pan *et al.*, 1997) but is not required for pol II binding (Awrey *et al.*, 1998) we think its effect on CB targeting reflects the interaction of TFIIS with another holoenzyme component that may or may not be associated simultaneously with pol II. In regard to the contribution of the C-terminal region, we think that reduction in CB targeting observed for the C-terminal deletion construct xIISΔ232 is due to the absence of the linker rather than the zinc ribbon. This conclusion rests on the behaviour of the site-specific

mutant xZR2 in which the two of the zinc-liganding cysteines essential for the structural integrity of the domain were substituted but the mutant nevertheless exhibited an apparently normal CB targeting efficiency. The conformationally flexible linker is involved in the interactions between TFIIS and the transcription complex, possibly by affecting the relative arrangements of pol II and TFIIS domains II and III (Olmsted *et al.*, 1998; Shimasaki and Kane, 2000). However, the strongest contribution to CB targeting was made by the region of TFIIS containing domain II itself, which is necessary and sufficient for pol II binding (Awrey *et al.*, 1998). The pol II interacting region within the domain contains a cluster of solvent-accessible lysines and arginines (Fig. 1) that are thought to form a basic patch on the surface of TFIIS. Mutation of these residues in yeast and human TFIIS reduces its pol II binding affinity and ability to stimulate *in vitro* transcription (Awrey *et al.*, 1998; Cipres-Palacin and Kane, 1995). We found that mutation of two of these basic residues in the xPOL2 mutant of *Xenopus* TFIIS reduced CB targeting efficiency and that the presence of the interacting region was also necessary for deletion constructs to show detectable CB targeting. Overall we conclude that the efficient CB targeting of TFIIS relies on a major interaction with pol II mediated by domain II together with a contribution from the linker region.

The site of binding by TFIIS to yeast pol II has been localized to a domain of the largest pol II subunit, RPB1, that is thought to be negatively charged (Wu *et al.*, 1996). This putative acidic patch on pol II may mediate an ionic interaction with the surface basic patch of the pol II-interaction domain of TFIIS (Awrey *et al.*, 1998). In addition there are genetic interactions between TFIIS and the pol II subunits RPB2 (Lennon *et al.*, 1998) and RPB6 (Ishiguro *et al.*, 2000). In the latter case there is also evidence of physical contact with TFIIS and it has been

suggested that TFIIS interacts with multimeric pol II at a surface formed by the three aforementioned pol II subunits (Ishiguro *et al.*, 2000). Although it is conceivable that CB targeting of TFIIS is brought about by its interaction with the acidic binding domain of free RPB1 subunits, given that other pol II subunits are also targeted to oocyte CBs (Morgan *et al.*, 2000), the fact that *in vitro* TFIIS is known to bind to intact, enzymatically-active pol II (Awrey *et al.*, 1998) and the putative involvement of multiple pol II subunits in generating the binding surface (Ishiguro *et al.*, 2000), it seems more likely that the target for the pol II binding activity of TFIIS in CBs is multimeric pol II. It would follow from this that rather than their being just sinks for the accumulation of free subunits of pol II and its transcription factors, CBs could indeed contain the full or partial pol II transcriptional assemblies predicted by the transcriptosome model (Gall *et al.*, 1999; Gall, 2000).

The subnuclear localization and targeting behaviour of TFIIS also make predictions regarding aspects of its *in vivo* function that extend and refine suggestions made from previous biochemical and genetic studies. First, TFIIS is present in two types of transcriptionally inert structures, CBs and chromosome granules, and this together with the requirement for pol II- and holoenzyme-binding regions in achieving efficient CB targeting, suggests that TFIIS is normally associated with the pol II transcriptional machinery when it is not engaged in elongation. The finding that the pol II holoenzyme purified by affinity chromatography with TFIIS is capable of initiating transcription has been interpreted as indicating that TFIIS may play a role in the initiation process (Pan *et al.*, 1997). The fact that TFIIS is also targeted as rapidly and efficiently to CBs as are pol II subunits (Morgan *et al.*, 2000) is again consistent with TFIIS and pol II being associated prior to the initiation of transcription. On the contrary, and perhaps at first sight

paradoxically, our data also suggest that in oocytes TFIIIS may not be associated with pol II during transcription elongation. We did not find specific immunostaining of lampbrush chromosome loops using a TFIIIS antiserum even though the intense staining of the much smaller chromosome granules shows that the approach had sufficient sensitivity and discrimination for the detection of TFIIIS in highly restricted chromosomal regions. Although it is conceivable that during transcription elongation the bulk of TFIIIS is somehow inaccessible to antibody binding in a way that it is not in the CBs and chromosome granules, targeting experiments with N-terminally epitope-tagged TFIIIS also failed to provide evidence for its presence either in the loops of lampbrush chromosomes from *Xenopus* or in the much longer loops of newt oocytes. Since it appears that *in vitro* TFIIIS interacts with template-engaged pol II with the same affinity as free pol II (Awrey *et al.*, 1998) the dynamic exchange of endogenous for tagged TFIIIS might be expected to lead to pol II elongation complexes being as efficiently targeted by TFIIIS as pol II complexes in CBs or chromosome granules. It should be noted however that the tagged pol II subunits RPB9 and RPB6 likewise are not targeted to loop axes in *Xenopus* and newt oocytes (Morgan *et al.*, 2000) although exchange of these integral parts of the polymerase during the process of transcription may be subject to different constraints than is TFIIIS.

Overall we conclude that TFIIIS is rarely, if ever, a component of the elongation complexes engaged in transcribing the oocyte genome. This conclusion is not incompatible with the long established *in vitro* activity of TFIIIS in stimulating elongation past sites of transcriptional arrest since TFIIIS could exhibit a “hit and run” mode of action in which it only binds to arrested transcription complexes. Even according to this scenario our finding of the apparent absence of TFIIIS from lampbrush loops would obviously require that the instances of TFIIIS interacting with

arrested pol II are few and far between, if they occur at all. This interpretation is supported by studies of lampbrush loop transcription using electron microscopy (Miller and Hamkalo, 1972; Scheer *et al.*, 1976) which reveal typical transcription units as long arrays of closely-packed, evenly-spaced transcription complexes without the extensive gaps that would result from arrested polymerases undergoing repeated TFIIS-induced attempts to recommence elongation. The high rates of initiation and levels of processivity exhibited by the lampbrush transcriptional apparatus appear to be correlated with unusual chromatin composition and levels of pol II CTD phosphorylation (reviewed in Morgan, 2002) and so the control of transcription elongation in lampbrush-stage oocytes could be regarded as highly atypical. However, recent experiments with yeast cells using chromatin immunoprecipitation assays have shown that under conditions of optimal growth TFIIS is not associated with either an activated gene or a constitutively transcribed gene (Pokholok *et al.*, 2002). When cells were subjected to stress conditions that reduced transcription elongation rates TFIIS did become associated with these genes, implying that *in vivo* TFIIS interacts with elongating pol II complexes only when elongation is compromised. The apparent absence of TFIIS from the maximally-active transcription units of lampbrush chromosomes supports this emerging view of the *in vivo* function of TFIIS as a conditional elongation factor.

#### ACKNOWLEDGEMENTS

We thank Drs. M. Jantsch, P. Labhart, M. Roth and Z. Wu for gifts of plasmid DNAs and Professors A. Lamond and J.G. Gall for antibodies. We are also extremely grateful to Joe Gall for communicating unpublished data and for help and advice that were essential for our

studies. This work was supported by a BBSRC studentship (AJS) and by a grant (053665) from the Wellcome Trust.

## REFERENCES

- Abbott, J., Marzluff, W.F., and Gall, J.G. (1999). The stem-loop binding protein (SLBP1) is present in coiled bodies of the *Xenopus* germinal vesicle. *Mol. Biol. Cell* *10*, 487-499.
- Awrey, D.E., Shimasaki, N., Koth, C., Weilbaecher, R., Olmsted, V., Kazanis, S., Shan, X., Arellano, J., Arrowsmith, C.H., Kane, C.M., and Edwards, A.M. (1998). Yeast transcript elongation factor (TFIIS), structure and function. II: RNA polymerase binding, transcript cleavage, and read-through. *J. Biol. Chem.* *273*, 22595-22605.
- Booth, V., Koth, C.M., Edwards, A.M., and Arrowsmith, C.H. (2000). Structure of a conserved domain common to the transcription factors TFIIS, elongin A, and CRSP70. *J. Biol. Chem.* *275*, 31266-31268.
- Bucci, S., Giani, L., Mancino, G., Pellegrino, M., and Raghianti, M. (2001). TAFII70 protein in Cajal bodies of the amphibian germinal vesicle. *Genome* *44*, 1100-1103.
- Callan, H.G. (1986). *Lampbrush Chromosomes*. Springer-Verlag: Berlin.
- Cipres-Palacin, G., and Kane, C.M. (1995). Alanine-scanning mutagenesis of human transcript elongation factor TFIIS. *Biochemistry* *34*, 15375-15380.
- Doyle, O., Corden, J.L., Murphy, C., and Gall, J.G. (2002). The distribution of RNA polymerase II largest subunit (RPB1) in the *Xenopus* germinal vesicle. *J. Struct. Biol.* *in press*.
- Dundr, M., and Misteli, T. (2001). Functional architecture in the cell nucleus. *Biochem. J.* *356*, 297-310.

Evan, G.I., Lewis, G.K., Ramsay, G., and Bishop, J.M. (1985). Isolation of monoclonal antibodies specific for human c-myc proto- oncogene product. *Mol. Cell. Biol.* *5*, 3610-3616.

Gall, J.G. (1992). Organelle assembly and function in the amphibian germinal vesicle. *Adv Devel Biochem* *1*, 1-29.

Gall, J.G. (2000). Cajal bodies: the first 100 years. *Ann. Rev. Cell Dev. Biol.* *16*, 273-300.

Gall, J.G., Bellini, M., Wu, Z., and Murphy, C. (1999). Assembly of the nuclear transcription and processing machinery: Cajal bodies (coiled bodies) and transcriptosomes. *Mol. Biol. Cell* *10*, 4385-4402.

Gall, J.G., and Murphy, C. (1998). Assembly of lampbrush chromosomes from sperm chromatin. *Mol. Biol. Cell* *9*, 733-747.

Gall, J.G., Murphy, C., Callan, H.G., and Wu, Z.A. (1991). Lampbrush chromosomes. *Methods Cell Biol* *36*, 149-166.

Gall, J.G., Tsvetkov, A., Wu, Z., and Murphy, C. (1995). Is the sphere organelle/coiled body a universal nuclear component? *Dev Genet* *16*, 25-35.

Harlow, E., and Lane, D. (1999). *Using antibodies. A laboratory manual.* Cold Spring Harbor Laboratory Press: Cold Spring Harbor, New York.

Hirose, Y., and Manley, J.L. (2000). RNA polymerase II and the integration of nuclear events. *Genes Dev.* *14*, 1415-1429.

Ishiguro, A., Nogi, Y., Hisatake, K., Muramatsu, M., and Ishihama, A. (2000). The Rpb6 subunit of fission yeast RNA polymerase II is a contact target of the transcription elongation factor TFIIS. *Mol. Cell. Biol.* *20*, 1263-1270.

Jantsch, M.F., and Gall, J.G. (1992). Assembly and localization of the U1-specific snRNP C protein in the amphibian oocyte. *J. Cell Biol.* *119*, 1037-1046.

Labhart, P. (1997). Transcript cleavage in an RNA polymerase I elongation complex. Evidence for a dissociable activity similar to but distinct from TFIIS. *J. Biol. Chem.* *272*, 9055-9061.

Labhart, P., and Morgan, G.T. (1998). Identification of novel genes encoding transcription elongation factor TFIIS (TCEA) in vertebrates: conservation of three distinct TFIIS isoforms in frog, mouse, and human. *Genomics* *52*, 278-288.

Lennon, J.C., 3rd, Wind, M., Saunders, L., Hock, M.B., and Reines, D. (1998). Mutations in RNA polymerase II and elongation factor SII severely reduce mRNA levels in *Saccharomyces cerevisiae*. *Mol. Cell. Biol.* *18*, 5771-5779.

Matera, A.G. (1999). Nuclear bodies: multifaceted subdomains of the interchromatin space. *Trends Cell Biol.* *9*, 302-309.

Miller, O.L., Jr., and Hamkalo, B.A. (1972). Visualization of RNA synthesis on chromosomes. *Int. Rev. Cytol.* *33*, 1-25.

Misteli, T. (2001). Protein dynamics: implications for nuclear architecture and gene expression. *Science* *291*, 843-847.

Morgan, G.T. (2002). Lampbrush chromosomes and associated bodies: new insights into principles of nuclear structure and function. *Chromosome Res.* *10*, 177-200.

Morgan, G.T., Doyle, O., Murphy, C., and Gall, J.G. (2000). RNA polymerase II in Cajal bodies of amphibian oocytes. *J. Struct. Biol.* *129*, 258-268.

Morin, P.E., Awrey, D.E., Edwards, A.M., and Arrowsmith, C.H. (1996). Elongation factor TFIIS contains three structural domains: solution structure of domain II. *Proc. Natl. Acad. Sci. U S A* *93*, 10604-10608.

Murphy, C., Wang, Z., Roeder, R.G., and Gall, J.G. (2002). RNA Polymerase III in Cajal bodies and lampbrush chromosomes of the *Xenopus* oocyte nucleus. *Mol. Biol. Cell* *13*, 3466-3476.

Myer, V.E., and Young, R.A. (1998). RNA polymerase II holoenzymes and subcomplexes. *J. Biol. Chem.* 273, 27757-27760.

Olmsted, V.K., Awrey, D.E., Koth, C., Shan, X., Morin, P.E., Kazanis, S., Edwards, A.M., and Arrowsmith, C.H. (1998). Yeast transcript elongation factor (TFIIS), structure and function. I: NMR structural analysis of the minimal transcriptionally active region. *J. Biol. Chem.* 273, 22589-22594.

Pan, G., Aso, T., and Greenblatt, J. (1997). Interaction of elongation factors TFIIS and elongin A with a human RNA polymerase II holoenzyme capable of promoter-specific initiation and responsive to transcriptional activators. *J. Biol. Chem.* 272, 24563-24571.

Plant, K.E., Hair, A., and Morgan, G.T. (1996). Genes encoding isoforms of transcription elongation factor TFIIS in *Xenopus* and the use of multiple unusual RNA processing signals. *Nucleic Acids Res.* 24, 3514-3521.

Pokholok, D.K., Hannett, N.M., and Young, R.A. (2002). Exchange of RNA polymerase II initiation and elongation factors during gene expression in vivo. *Mol. Cell* 9, 799-809.

Qian, X., Gozani, S.N., Yoon, H., Jeon, C.J., Agarwal, K., and Weiss, M.A. (1993). Novel zinc finger motif in the basal transcriptional machinery: three-dimensional NMR studies of the nucleic acid binding domain of transcriptional elongation factor TFIIS. *Biochemistry* 32, 9944-9959.

Robert, F., Blanchette, M., Maes, O., Chabot, B., and Coulombe, B. (2002). A human RNA polymerase II-containing complex associated with factors necessary for spliceosome assembly. *J. Biol. Chem.* 277, 9302-9306.

Scheer, U., Franke, W.W., Trendelenburg, M.F., and Spring, H. (1976). Classification of loops of lampbrush chromosomes according to the arrangement of transcriptional complexes. *J. Cell Sci.* 22, 503-519.

Shimasaki, N.B., and Kane, C.M. (2000). Structural basis for the species-specific activity of TFIIS. *J. Biol. Chem.* 275, 36541-36549.

Taira, Y., Kubo, T., and Natori, S. (1998). Molecular cloning of cDNA and tissue-specific expression of the gene for SII-K1, a novel transcription elongation factor SII. *Genes Cells* 3, 289-296.

Taira, Y., Kubo, T., and Natori, S. (2000). Participation of transcription elongation factor XSII-K1 in mesoderm- derived tissue development in *Xenopus laevis*. *J. Biol. Chem.* 275, 32011-32015.

Tuma, R.S., Stolk, J.A., and Roth, M.B. (1993). Identification and characterization of a sphere organelle protein. *J. Cell Biol.* 122, 767-773.

Warren, S.L., Landolfi, A.S., Curtis, C., and Morrow, J.S.W. (1992). Cytostellin: a novel, highly conserved protein that undergoes continuous redistribution during the cell cycle. *J. Cell Sci.* 103, 381-388.

Wind, M., and Reines, D. (2000). Transcription elongation factor SII. *Bioessays* 22, 327-336.

Wu, J., Awrey, D.E., Edwards, A.M., Archambault, J., and Friesen, J.D. (1996). In vitro characterization of mutant yeast RNA polymerase II with reduced binding for elongation factor TFIIS. *Proc. Natl. Acad. Sci. U S A* 93, 11552-11557.

Wu, Z., Murphy, C., and Gall, J.G. (1994). Human p80-coilin is targeted to sphere organelles in the amphibian germinal vesicle. *Mol. Biol. Cell* 5, 1119-1127.

## FIGURE LEGENDS

Fig. 1. Domain organization and sequence conservation of TFIIIS.

At the top is a diagram of the domain organization of yeast TFIIIS (yTFIIIS). The amino acid residues corresponding to the three domains (I, II and III) defined by limited proteolysis, are indicated on the diagram. Functions so far determined for these domains are indicated above (Wind and Reines, 2000), while below are indicated the structural domains identified by NMR spectroscopy (Olmsted *et al.*, 1998; Booth *et al.*, 2000). In the centre is a summary of the sequence organization of *Xenopus laevis* TFIIIS (xTFIIIS). Indicated are the amino acid residues defining the boundaries of those regions N, L and C, which exhibit distinctive levels of sequence conservation and are used here as the basis of deletion constructs. Below the diagram are indicated the inter-isoform amino acid sequence identities for each region, calculated as percentages by comparing xTFIIIS.o to the most diverged of the three vertebrate isoforms, xTFIIIS.h. One part of the region of lowest sequence conservation, L, exhibits some inter-isoform similarity while the other part is so distinctive in length and sequence that it is not alignable (na). Regions of yeast and /or vertebrate TFIIIS that are involved in macromolecular interactions (Wind and Reines, 2000) are indicated by bars above the diagram.

At the bottom of the figure are shown the residues comprising the third helix of domain II of yeast, human and *Xenopus* TFIIIS that are thought to mediate the binding of TFIIIS to pol II (Awrey *et al.*, 1998). The basic residues substituted in this and other studies are shown as follows: for yTFIIIS, the underlines correspond to three single mutants constructed by Awrey *et al.* (1998), for hTFIIIS the single underlines correspond to the double mutant (“cluster 7”) and the

double underlines indicate the triple mutant (“cluster 7b”) of Ciprés-Palacín and Kane (1995) and for xTFIIS the underlines mark the residues substituted in the double mutant (“xPOL2”) constructed here.

Fig. 2. *Xenopus* TFIIS.o is recognised by serum 37X.

(A) Immunoblot of HeLa cell extracts probed with serum 37X. Extracts were obtained from cells that had been transfected with *myc*-tagged xTFIIS.o expression constructs encoding the regions of the polypeptide indicated by the amino acid co-ordinates above the lanes. Bands corresponding to *myc*-tagged xTFIIS.o were seen only for those constructs encoding the 80 amino acid N-terminal region against which the antibody was raised.

(B) Immunoblot of proteins from GVs manually isolated from 5 uninjected oocytes (un) and from the same number of oocytes injected 24 h previously with transcripts encoding *myc*-tagged xTFIIS.o or xTFIIS.l. In all of the GV extracts a band at about 35 kDa (arrowhead) corresponds to the size expected for endogenous xTFIIS.o. A major band corresponding to full-length *myc*-tagged xTFIIS.o (arrow) as well as some minor degradation products is also detected in extracts of injected oocytes but xTFIIS.l is not detectable.

Fig. 3 Localization of TFIIS.o in *Xenopus* GV spreads.

Images obtained by immunofluorescence are grouped with the corresponding DIC image.

(A) Immunostaining with serum 37X against xTFIIS.o produces brightly stained CBs (arrowhead) while other GV structures are only faintly stained. A weakly-stained B-snurposome-like inclusion body in the CB causes an off-centre “hole” in the CB matrix staining.

(B) Immunostaining with serum  $\alpha$ p80 against the CB marker protein, coilin demonstrates that the pattern of CB matrix staining (arrowhead) obtained with coilin antibodies is similar to that shown in (A) for TFIIS.

(C) Immunostaining with serum 37X also identifies a class of chromosomally-localized granules as sites of TFIIS accumulation. The arrows mark two terminal granules present at homologous loci at the end of a lampbrush chromosome bivalent.

(D) Double immunostaining of CBs (arrowheads) with mAb H14 against the phosphorylated CTD and with serum 37X shows that pol II and TFIIS are co-localized.

(E) Double staining of lampbrush chromosomes with mAb H14 and serum 37X. The transcriptionally-active axes of lampbrush loops (e.g. black arrowhead) are intensely stained for pol II but not for TFIIS. Co-localization of pol II and TFIIS is shown for the nearby CB (white arrowhead), in which TFIIS staining is even more intense than pol II staining.

B, B snurposome; N, nucleolus. Scale bars represent 10  $\mu$ m.

Fig. 4 Expression and targeting of *myc*-tagged xTFIIS.o in *Xenopus* oocytes.

(A) Immunoblot of extracts, each equivalent to 5 GVs, prepared from oocytes injected 4 h or 8 h previously with *myc*-xIIS transcripts. Also blotted were *in vitro* translation products (ivt) from the same transcripts. The blot was probed with mAb 9E10 against the *myc* tag and shows the presence in all samples of a major band at about 50 kDa.

(B) Rapid targeting of *myc*-tagged TFIIS to CBs. In GV spreads of oocytes injected as in (A) all CBs (arrowheads in the DIC images) were strongly stained by mAb 9E10 after incubation for periods as short as 4 to 8 h. The other spherical objects visible in these images are B snurposomes, which exhibit much less staining.

(C) Immunofluorescent staining of GV spreads either from oocytes injected with *myc*-xIIS or from uninjected control oocytes that were both incubated in parallel for 48 h. Spreads were co-stained with mAb 9E10 and serum  $\alpha$ p80 against coilin. CBs (arrowheads) from injected oocytes showed strong staining for the *myc* epitope while nucleoli (N) lampbrush chromosomes (LBC) and B snurposomes (B), including those attached to CBs, were much more weakly stained.

(D) Targeting of TFIIIS to chromosome granules. Part of a lampbrush chromosome isolated from an oocyte injected 24 h previously with a UTR-containing transcript encoding *myc*-tagged TFIIIS and stained with mAb 9E10. As well as CBs (white arrowhead), chromosome granules such as the homologous terminal granules shown (black arrowheads) were distinctly stained.

All scale bars represent 10  $\mu$ m.

Fig. 5 Targeting of *myc*-tagged xTFIIIS.o to CBs in *Triturus* GVs.

*myc*-xTFIIIS transcripts containing the UTR and coding region were injected into the cytoplasm of oocytes from the newt, *Triturus vulgaris* and GV spreads made 24 h later. The upper image shows the detection of tagged TFIIIS by immunofluorescence using mAb 9E10. CBs were intensely stained including, as shown here (white arrowhead in the phase contrast image below), an extremely large example that is regularly attached at a specific site on lampbrush chromosome VI. There is much weaker staining of the equally massive “lumpy loop” structures (black arrowhead) proximal to the CB and of the RNP matrices of typical loops. Also shown is an example of the anti-*myc* staining pattern obtained in *T. vulgaris* GV spreads after expression in oocytes of a *myc*-tagged fusion of the U1-snRNP-specific “C” protein (Jantsch and Gall, 1992). Lateral loop matrices are strongly stained whereas the chromosomally-attached CB (white arrowhead in the phase contrast image below) is relatively weakly stained.

Scale bar represents 10 $\mu$ m.

Fig. 6. No single region of TFIIIS is responsible for efficient CB targeting.

(A) A series of *myc*-tagged deletion constructs based on the regions of xTFIIIS detailed in Fig. 1.

Regions are labelled and shaded as in Fig 1 and each construct contains an SV40 nuclear localization signal (nls). Summarised on the right is the extent of CB targeting observed by immunostaining GV spreads from *Xenopus* oocytes injected with each deletion construct or with full-length *myc*-xIIS. The relative staining intensities of CBs was estimated with respect to the background staining exhibited by attached or neighbouring B snurposomes as follows: +++, strong CB staining; + weak but specific CB staining; -, no specific CB staining.

(B) Immunoblot of GV extracts taken from oocytes injected with transcripts encoding each of the deletion constructs. After probing with mAb 9E10 full-length bands of the expected size were seen together with degradation products in the case of constructs containing the L region.

(C) Immunofluorescent co-staining with mAb 9E10 and anti-coilin antiserum of GV spreads prepared in parallel with the GV extracts in (B) from oocytes injected with a deletion construct or with full-length *myc*-xIIS. All images were captured under the same conditions from the same injection series using a single batch of oocytes and utilise the full range of gray-scale values.

Scale bar represents 10  $\mu$ m.

Fig. 7. A C-terminal but not an internal deletion reduces CB targeting by TFIIIS.

(A) Two *myc*-tagged mutant constructs derived by deletion either of the internal L region of xIIS or of the C-terminal 71 amino acids of the UTR-xIIS fusion. On the right is a summary of the

extent of CB targeting observed for either deletion construct or the full-length parental construct in immunostained GV spreads from injected *Xenopus* oocytes. The relative *myc* staining intensities of CBs were estimated with respect to the background staining exhibited by attached or neighbouring B snurposomes as follows: +++++, very strong CB staining (typical of full length UTR-containing constructs); +++, normal, strong CB staining; ++ reduced CB staining.

(B) Immunofluorescent staining with mAb 9E10 of CBs (arrowheads) from oocytes expressing either the L-region deletion construct, xN+C or the full-length parental construct, xIIS. The *myc* staining of CBs (arrowheads in the DIC images below) appears similar for both constructs.

(C) Reduced mAb 9E10 staining of CBs (arrowheads) from oocytes expressing the C-terminal deletion construct, myc-UTR-xIIS $\Delta$ 232, compared to the full-length parental construct, myc-UTR-xIIS. Saturation of the immunofluorescent image evident in the CB for UTR-xIIS is a consequence of imaging the B snurposome background at similar levels in this figure. Scale bar represents 10  $\mu$ m.

Fig. 8. Site-specific mutation of the xTFIIS pol II binding region reduces CB targeting.

(A) Site-specific mutants constructed by substitution of residues in three conserved sequence motifs of myc-xIIS. The approximate locations of the mutations in xTFIIS are indicated by asterisks above each diagram and the residues substituted are indicated below them. On the right is a summary of the extent of CB targeting observed for each mutant or for wild type xIIS in immunostained GV spreads from injected *Xenopus* oocytes. The relative *myc* staining intensities of CBs were estimated with respect to the background staining exhibited by attached or neighbouring B snurposomes; the strong staining normally found for xIIS (+++) was also found

for two mutants, but for the myc-xPOL2 mutant specific CB staining varied between appearing somewhat reduced (++) to being undetectable (-).

(B) Immunofluorescent co-staining with mAb 9E10 and anti-coilin antiserum of GV spreads prepared 24 h after oocytes had been injected with transcripts of site-specific mutants or wild type myc-xIIS. The images were captured under the same conditions from the same injection series and each utilises the full range of gray-scale values.

(C) The variable reduction in targeting to CBs (arrowheads) exhibited by the xPOL2 mutant is shown in GV spreads prepared from a further two oocyte injection series, i and ii, in both of which oocytes were incubated for 48 h after injection. Control spreads prepared from oocytes injected in parallel with the wild type xIIS are also shown.

Scale bars represent 10  $\mu\text{m}$ .

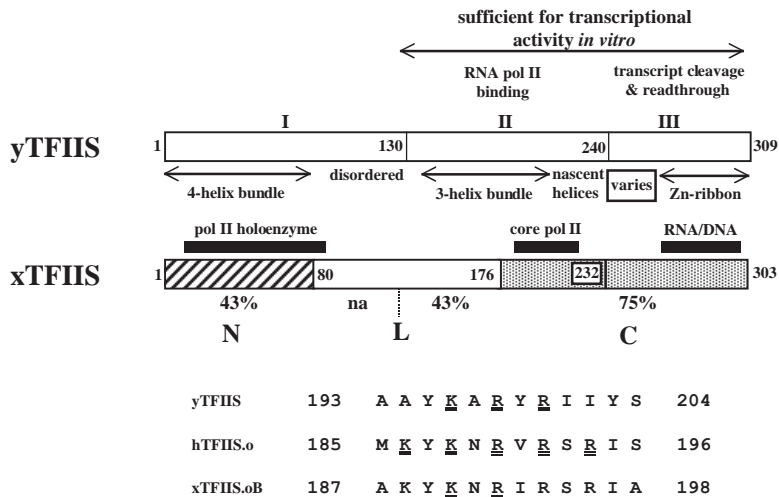
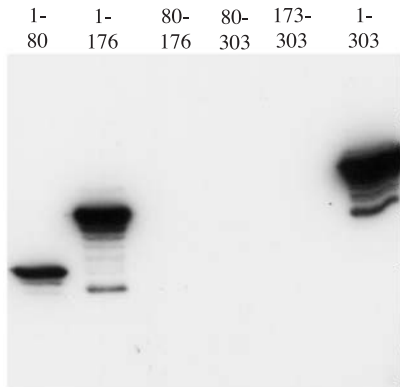


Fig. 1

A



B

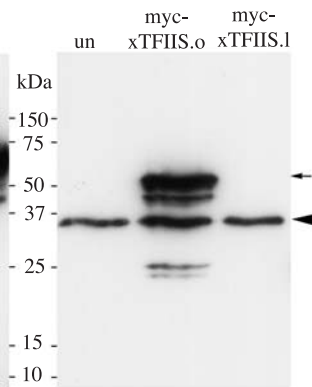


Fig. 2

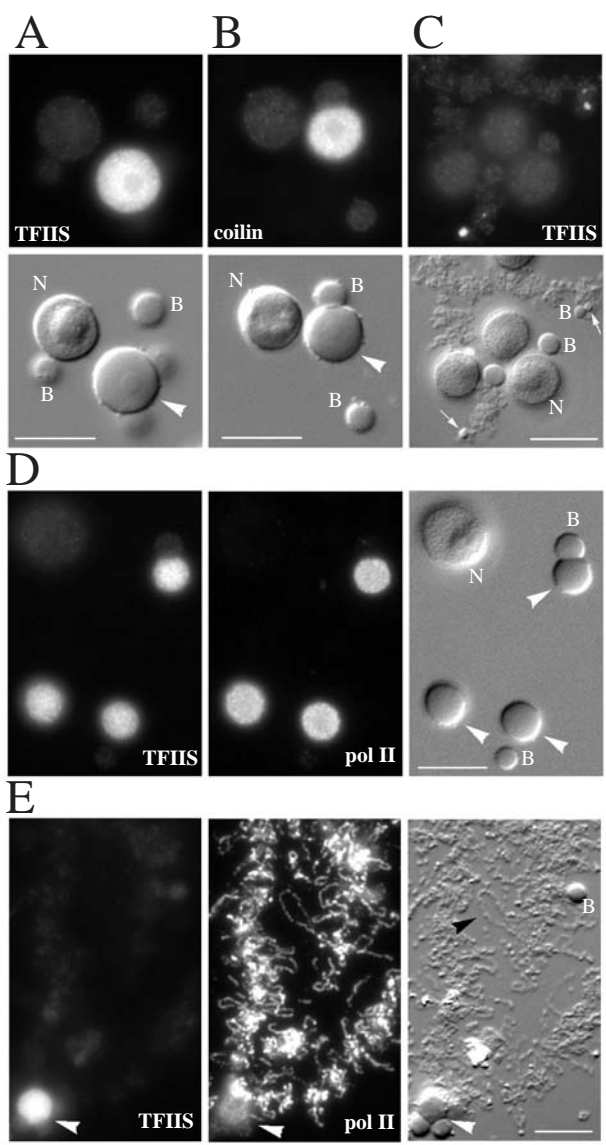


Fig. 3

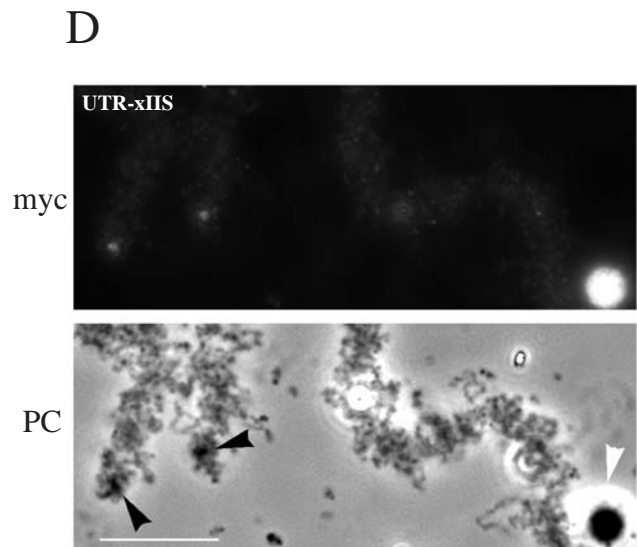
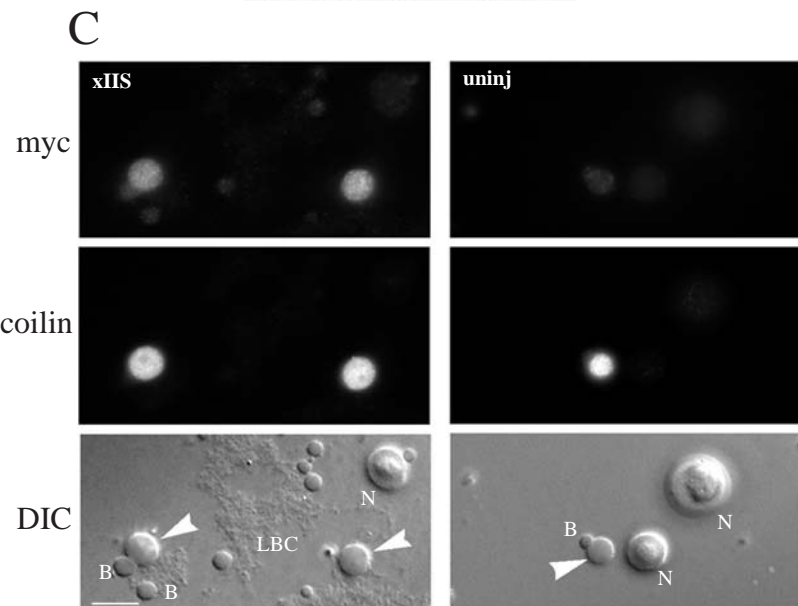
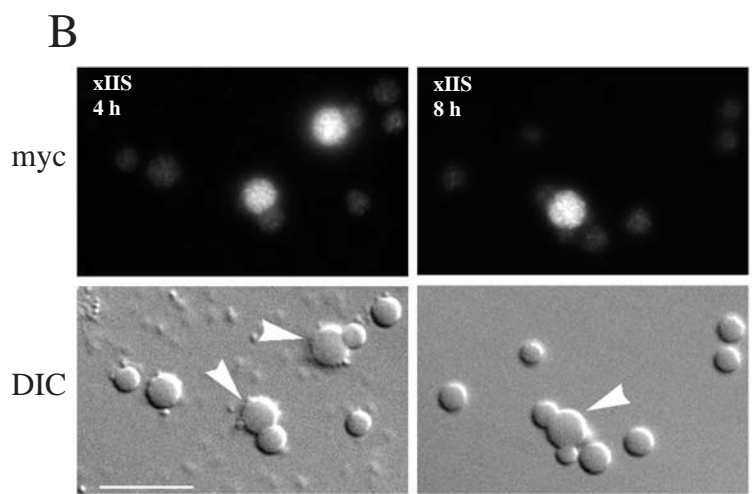
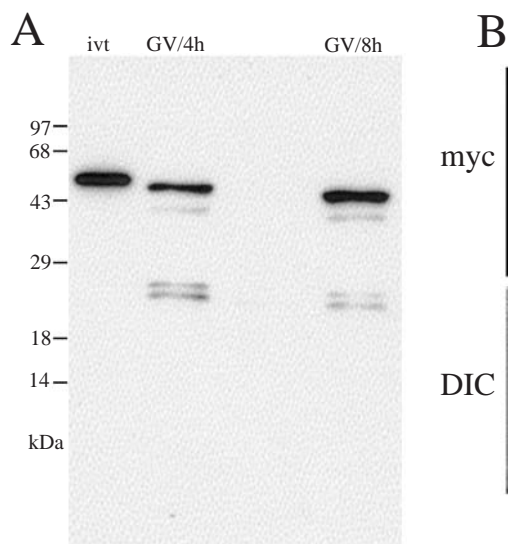


Fig. 4

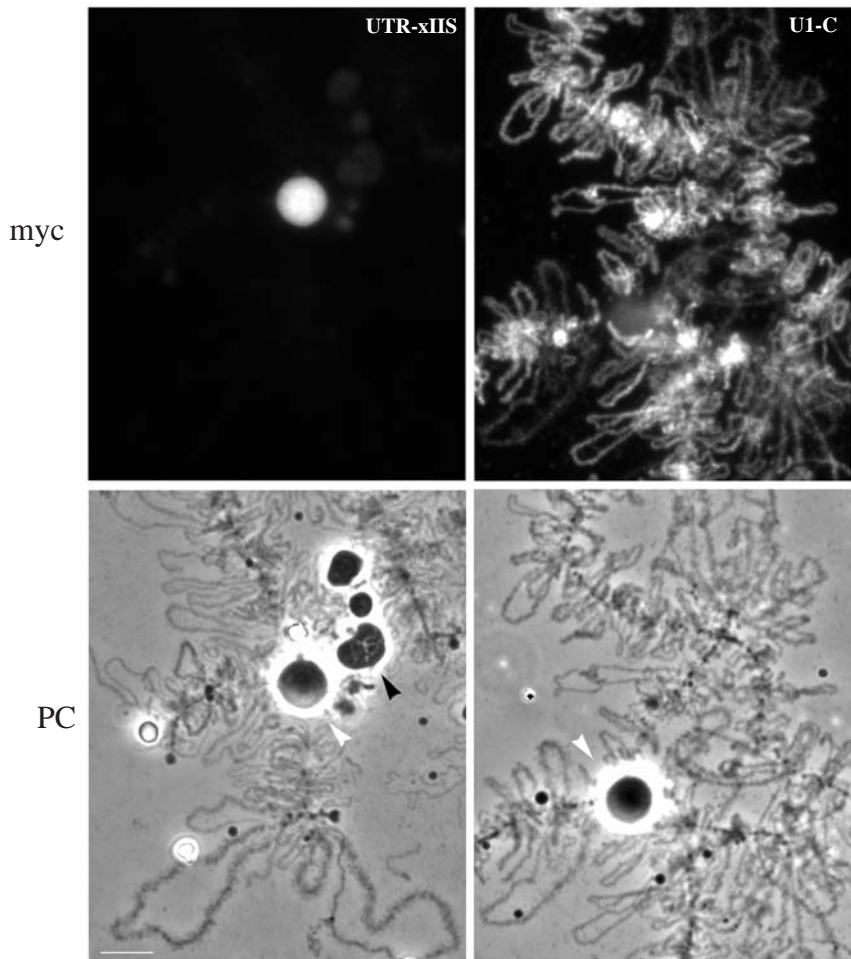
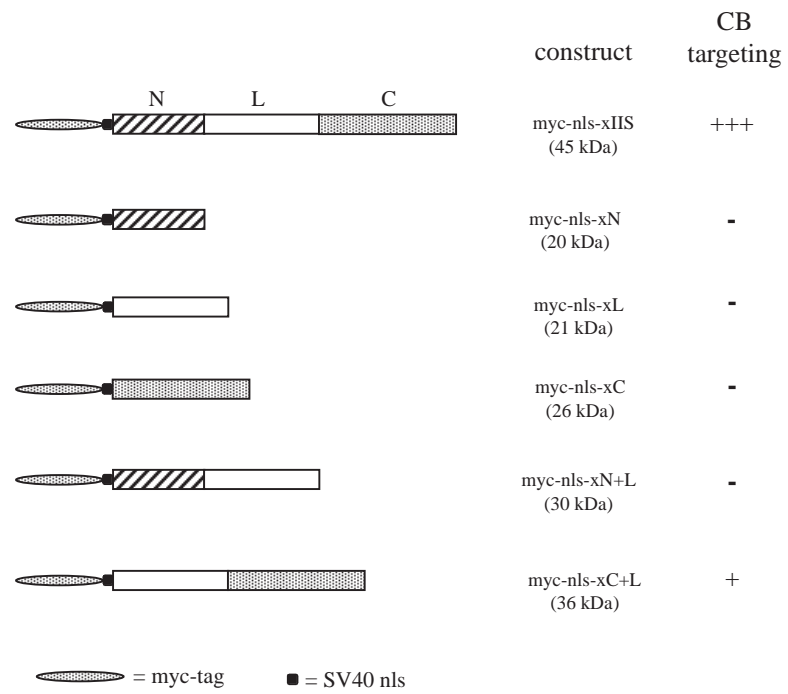
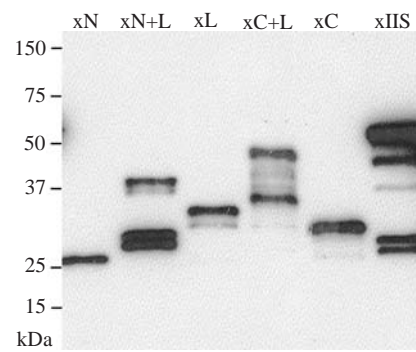


Fig. 5

A



B



C

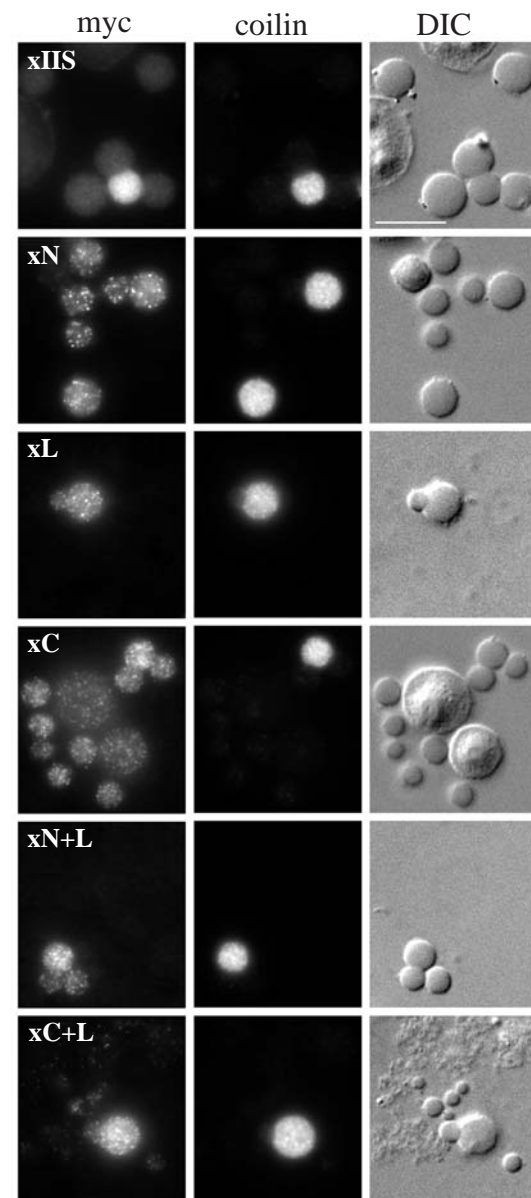


Fig. 6

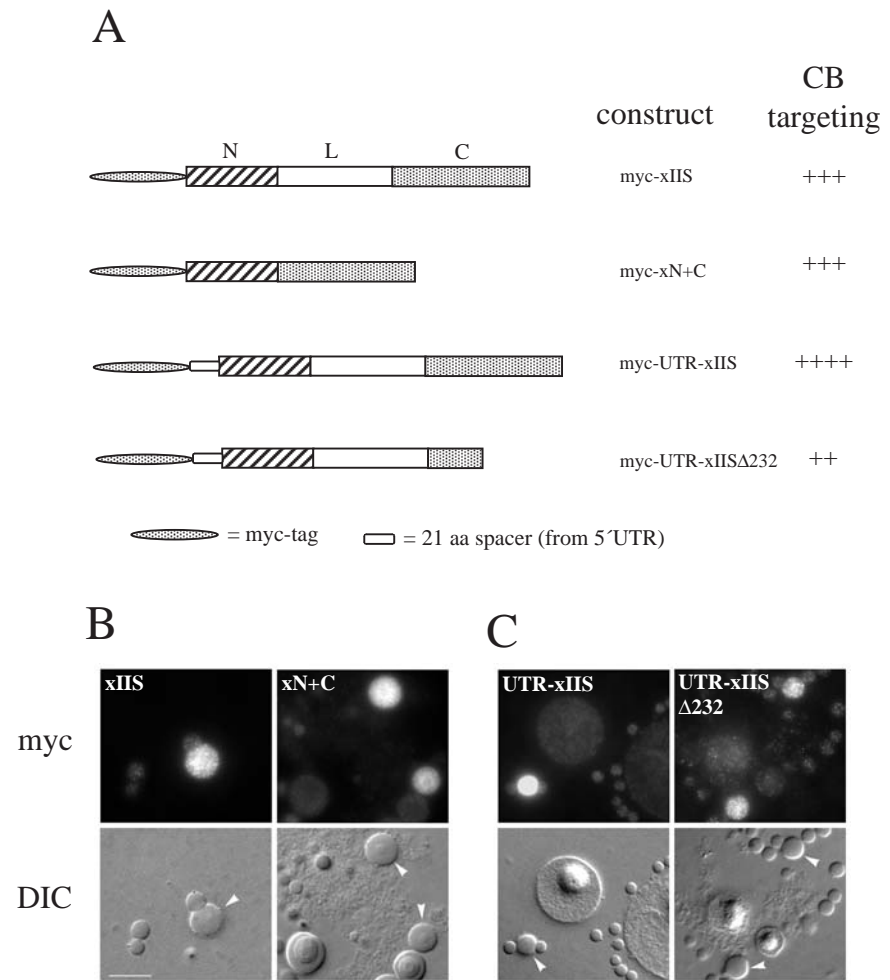
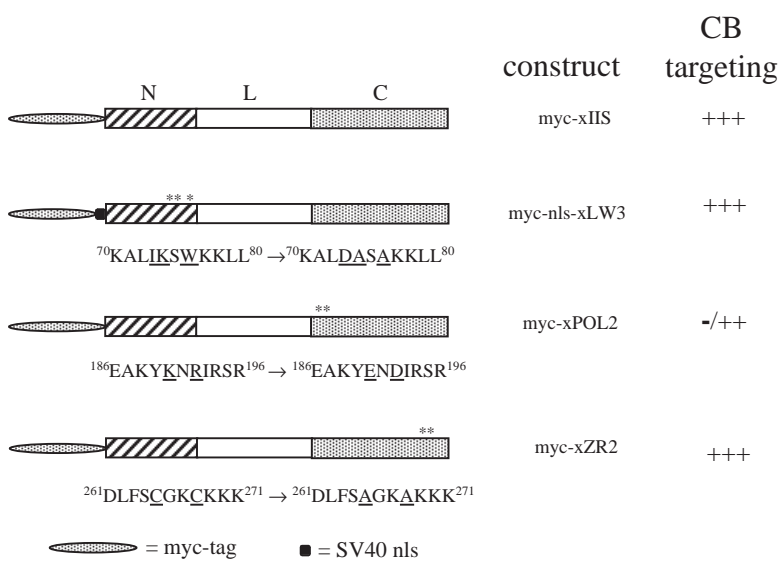
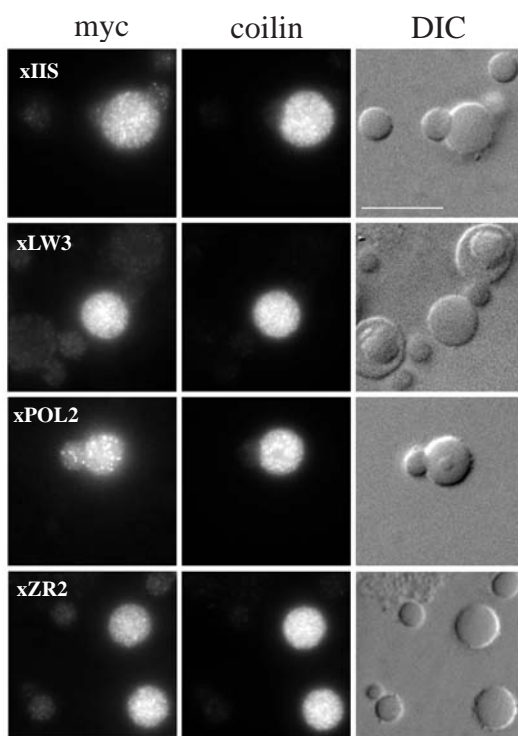


Fig. 7

A



B



C

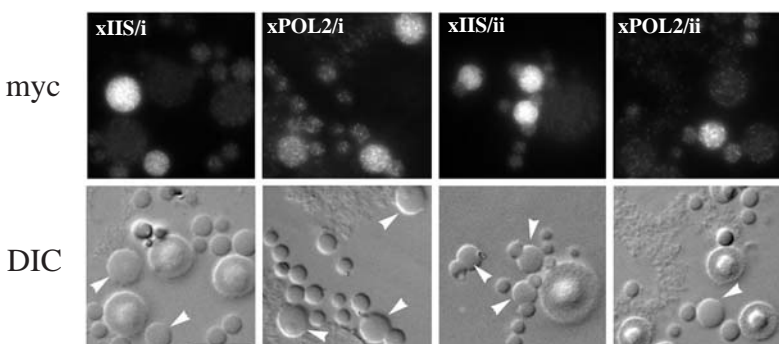


Fig. 8